Research Square

Preprints are preliminary reports that have not undergone peer review.
They should not be considered conclusive, used to inform clinical practice,
or referenced by the media as validated information.

Microbial community context shapes the evolutionary outcome of bacteria evolved on tomato plants

Tiffany Batarseh

t.batarseh@berkeley.edu

University of California Berkeley https://orcid.org/0000-0002-2271-0156

Fiona Wagner

University of California Berkeley

Rocelia Alvarez-Navarrete

University of California Berkeley

Chuyu Wang

University of California Berkeley

Jose Collado

University of California Davis

Britt Koskella

University of California, Berkeley https://orcid.org/0000-0003-1760-8496

Article

Keywords:

Posted Date: September 21st, 2026

DOI: https://doi.org/10.21203/rs.3.rs-10720469/v1

License: This work is licensed under a Creative Commons Attribution 4.0 International License.
Read Full License

Additional Declarations: There is **NO** Competing Interest.

Microbial community context shapes the evolutionary outcome of bacteria evolved on tomato plants

Tiffany N. Batarseh[1,2,*], Fiona J. Wagner[1], Rocelia Alvarez-Navarrete[1], Chuyu Wang[1], Jose O. Collado[1,3], Britt Koskella[1,2]

[1] Department of Integrative Biology, University of California Berkeley, Berkeley, CA, USA

[2] San Francisco Chan Zuckerberg Biohub, San Francisco, CA, USA

[3] Department of Nutrition, University of California Davis, Davis, CA, USA

*Corresponding author:

Tiffany N. Batarseh, Integrative Biology University of California Berkeley, 3060 Valley Life Sciences Building, Berkeley, CA, 94720, United States t.batarseh@berkeley.edu

ABSTRACT

Host-associated bacteria must adapt to their host while also facing selection from the microbiome, yet most evolution studies ignore the resident community. We experimentally evolved three *Pseudomonas* species spanning distinct ecological roles, the foliar pathogen *P. syringae*, the opportunist *P. moraviensis*, and the candidate growth-promoting *P. rhodesiae*, through 12 passages on tomato seedlings, alone or alongside a 14-member synthetic community. Relaxing competition in monoculture improved in vitro growth in two of three species, but these gains did not translate uniformly in planta: monoculture-evolved *P. syringae* caused less disease and colonized less well, polyculture-evolved *P. rhodesiae* colonized better across independent seedling and greenhouse assays, and *P. moraviensis* showed no phenotypic change. Whole-genome sequencing of all 36 populations identified 2,482 mutations across 101 independently mutated loci. Community context reshaped the molecular basis of adaptation: monoculture drove more complete selective sweeps (12.7% vs. 6.9% of mutations fixed), whereas polyculture populations retained twice as much standing variation (84 vs. 42 segregating mutations per population) and enriched genic mutations and hypermutator lineages in all three species. Both the ecological role of a bacterium and the community context in which it evolved leave a lasting imprint on evolutionary trajectories along the pathogen-to-mutualist continuum.

For host-associated bacteria, evolution is shaped by two potentially opposing forces: selection imposed by the host and selection imposed by other members of the microbiome. A colonizing lineage must adapt to the physical and immune environment of its host while also navigating competition, exploitation, or facilitation from the microbes sharing that niche. Because these pressures can pull in different directions, the adaptive trajectory of any one lineage is difficult to anticipate from either force alone[1–3]. Yet most of what we know about bacterial host adaptation comes from pairwise experiments conducted in the absence of the resident microbiome[4–6], and the few studies that do include a community show it can suppress or redirect adaptation[7–9], leaving unresolved whether the magnitude and direction of community-mediated evolutionary change depend on a focal species' own ecological role. The phyllosphere is a tractable system for testing this: a discrete, spatially separated habitat with a resident community stable enough to be defined, removed, and reconstituted experimentally[10–12], where synthetic communities (SynComs) have been successfully leveraged and preserve key microbial interactions while retaining experimental reproducibility[13].

Pseudomonas spans the full range of ecological roles in this habitat, from pathogen to plant growth-promoting bacterium (PGPB)[14], making it well suited to test whether ecological role predicts evolutionary response. We evolved three species representing distinct positions on this continuum: the pathogen *P. syringae*, the commensal *P. moraviensis* and the plant growth promoting *P. rhodesiae*. *P. syringae* pv. tomato DC3000 is a well-characterized foliar pathogen that causes bacterial speck disease and relies on a type III secretion system to suppress host immunity[15,16]. *P. rhodesiae* occupies the beneficial end of the gradient, with strains acting as biocontrol agents through induction of systemic resistance [17] and root architecture modification[18], supporting its assignment as a candidate PGPB. *P. moraviensis* occupies an

ambiguous position: classified as plant growth-promoting with substantial metabolic versatility[19,20], yet also implicated as an opportunistic, symptom-associated colonizer in diseased tissue[21,22]. Together these species allow ecological role to be varied while host, community, and evolutionary conditions are held constant.

We experimentally evolved all three species through 12 passages on tomato seedlings, either as monocultures or alongside a constant 14-member SynCom (**Figure 1** and **Table 1**), then characterized evolved populations across in vitro growth, in planta colonization and virulence, and whole-genome signatures of selection. We asked whether: (1) community presence predictably shapes phenotypic evolution based on ecological role of the focal bacterium; (2) microbial community presence alters the genotypic targets of selection and/or rate of molecular evolution; and (3) ecological role of the focal bacterium predicts the magnitude and direction of community-mediated selection. We find that while release from competition drives faster in vitro growth in two of three species, these gains did not translate consistently to growth on the host plant (where evolution occurred). While monoculture-evolved *P. syringae* lost virulence over the experiment, polyculture-evolved *P. rhodesiae* became the strongest plant colonizer, and *P. moraviensis* changed little on either axis. Community context also reshaped the molecular landscape of all three species by lowering fixation rates, enriching genic mutations, and promoting hypermutator lineages.

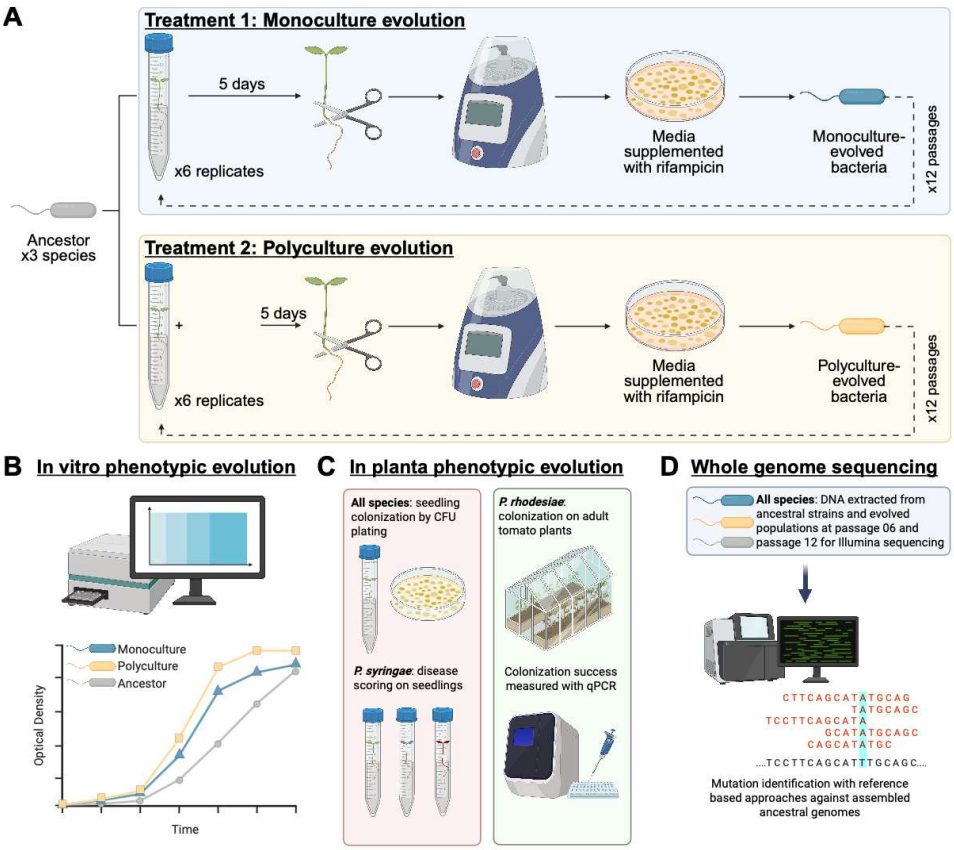


Figure 1. Schematic of the experimental evolution design used to study the effects of biotic interactions on *Pseudomonas* phenotypic and genotypic evolution. A) Three ancestral *Pseudomonas* species (*P. syringae* DC3000, *P. moraviensis* SC16, and *P. rhodesiae* SC25) evolved for 12 serial passages on 12-day-old tomato (*Solanum lycopersicum* cv. 'Moneymaker') seedlings under two treatments: monoculture (focal species alone) or polyculture (focal species co-inoculated with a 14-member synthetic community, SynCom). Six replicate lines were maintained per species per treatment (36 lines total). At each passage, seedlings were homogenized and re-inoculated onto fresh seedlings after selection on rifampicin-supplemented agar. Evolved populations were archived at each passage in -80.0°C freezer stocks. B) In vitro phenotypic evolution was assessed by growth curve analysis (OD_{600}) of ancestral, monoculture-evolved, and polyculture-evolved lines over 72 hours. C) In planta phenotypic evolution was assessed by seedling colonization by colony forming unit (CFU) plating for all three species, and by disease progression scoring on seedlings for *P. syringae*, the only pathogenic species among the three. For *P. rhodesiae*, which showed a significant colonization advantage in the seedling assay, colonization of adult tomato plants in the greenhouse was further assessed by qPCR. D) Whole-genome sequencing was performed on ancestral strains and evolved populations at Passage 6 and Passage 12 for all three species, with mutation identification performed against assembled ancestral reference genomes. Created in BioRender (https://BioRender.com/0mdg15w).

Table 1 Bacterial strains included in this study

Strain Identifier	Genus	Species	Role	Treatment
SC01	*Frigoribacterium*	*endophyticum*	SynCom member	Polyculture only
SC02	*Pantoea*	*agglomerans*	SynCom member	Polyculture only
SC03	*Curtobacterium*	*herbarum*	SynCom member	Polyculture only
SC04	*Erwinia*	*tasmaniensis*	SynCom member	Polyculture only
SC06	*Brevibacterium**	*frigoritolerans*	SynCom member	Polyculture only

SC09	*Massilia*[1]	*aurea*	SynCom member	Polyculture only
SC10	*Pseudomonas*	*asturiensis*	SynCom member	Polyculture only
SC13	*Exiguobacterium*	*sibiricum*[2]	SynCom member	Polyculture only
SC14	*Pseudomonas*	*rhizosphaerae*	SynCom member	Polyculture only
SC16	*Pseudomonas*	*moraviensis*	Ancestor	Both
SC21	*Rathayibacter*	*festucae*	SynCom member	Polyculture only
SC23	*Curtobacterium*	*pusillum*	SynCom member	Polyculture only
SC25	*Pseudomonas*	*rhodesiae*	Ancestor	Both
SC26	*Pantoea*	*allii*	SynCom member	Polyculture only
SC33	*Microbacterium*	*oleivorans*	SynCom member	Polyculture only
SC35	*Bacillus*	*thuringiensis*	SynCom member	Polyculture only
DC3000	*Pseudomonas*	*syringae*	Ancestor	Both

*Synonymous with *Peribacillus*
[1]Synonymous with *Telluria*
[2]Synonymous with *Exiguobacterium artemiae*

RESULTS

Phenotypic outcomes varied by species and evolution treatment on tomato seedlings

We evolved 3 species of *Pseudomonas* on tomato plant hosts for twelve passages, or roughly 40 bacterial generations, under two treatments: monoculture inoculations or polyculture inoculations with a constant synthetic microbial community (SynCom) of 14 species (**Figure 1**). Across both *P. rhodesiae* and *P. syringae*, monoculture-evolved lines (i.e. those released from microbial competition during the evolution experiment) outperformed their ancestor strain with faster per-capita growth, higher AUC, and/or higher maximum density in their growth curves (**Figure 2** and **Extended Data Table 1**).

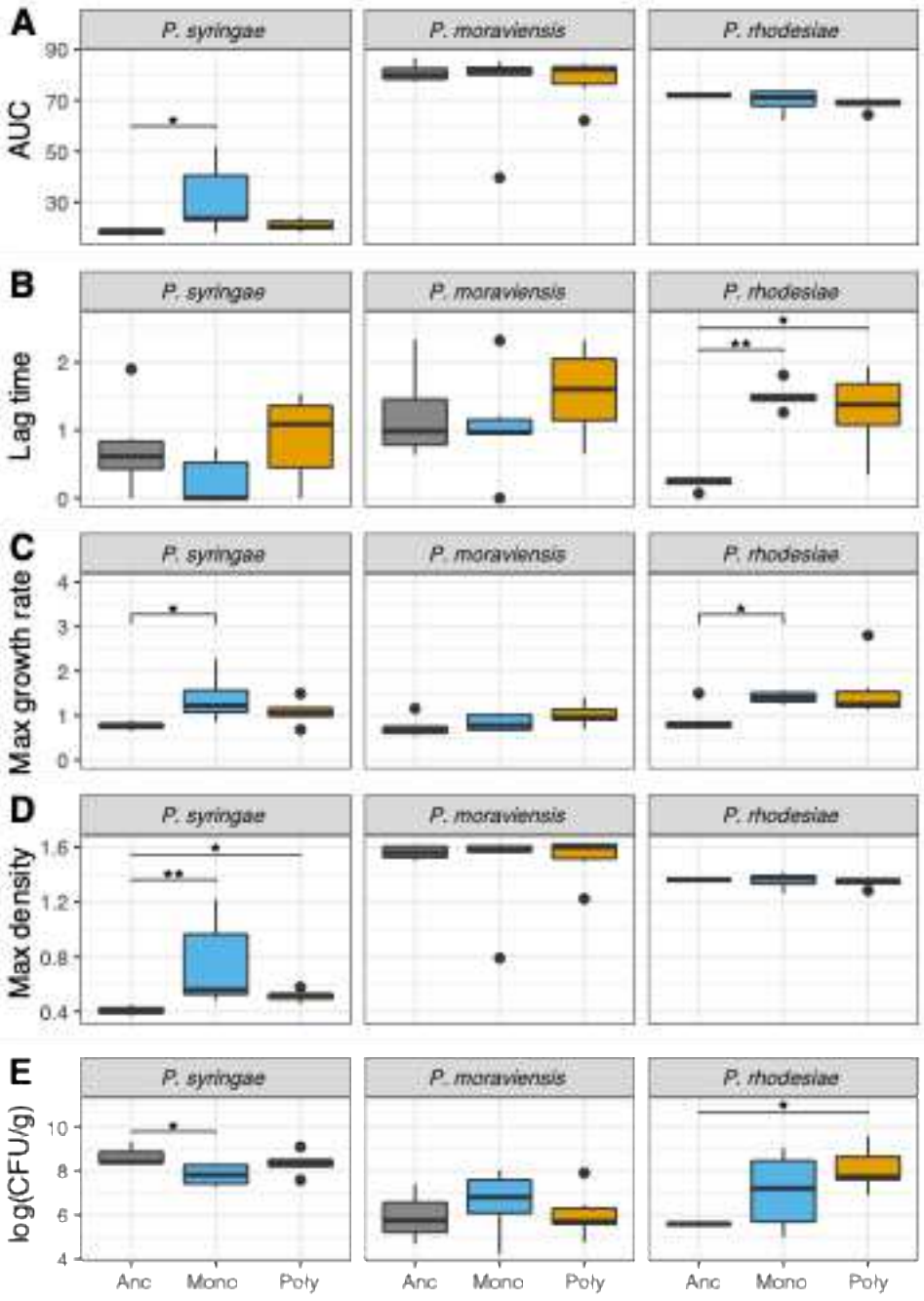


Figure 2. Changes in growth dynamics of ancestral (Anc) and monoculture (Mono) or polyculture (Poly) evolved Pseudomonas lines. A-D) In vitro growth curves were measured in liquid medium at 28.0°C for 72 hours (OD_{600} every 15 min). Four metrics are shown for each of the three focal species: area under the curve (AUC), lag time, maximum per-capita growth rate, and maximum density. E) In planta bacterial cell densities of ancestral and evolved Pseudomonas lines on tomato seedlings. Ancestral, monoculture-evolved, and polyculture-evolved lines were individually inoculated onto 12-day-old tomato seedlings and harvested after 5 days. Bacterial densities were quantified by serial dilution plating on rifampicin-supplemented agar. Points represent the average value for 3 technical replicates of each evolved line (n = 6 biological replicates per treatment) or ancestor; boxes show median and interquartile range. Statistical comparisons used Kruskal–Wallis tests with Dunn's post-hoc pairwise contrasts (Bonferroni-corrected); significant comparisons are indicated (* $p < 0.05$, ** $p < 0.01$).

P. syringae displayed the broadest pattern of in vitro growth improvement. Monoculture-evolved lines exhibited significantly higher AUC than ancestors (Kruskal-Wallis $\chi^2 = 7.83$, $p = 0.020$; Dunn's: monoculture vs. ancestor $p = 0.009$), faster maximum per-capita growth rate (KW $\chi^2 = 8.84$, $p = 0.012$; Dunn's: monoculture vs. ancestor $p = 0.005$), and greater maximum density (KW $\chi^2 = 12.12$, $p = 0.002$; Dunn's: monoculture vs. ancestor $p = 0.001$, polyculture vs. ancestor $p = 0.019$). Growth improvements were most pronounced in monoculture-evolved lines, with polyculture-evolved lines showing intermediate or comparable performance to ancestors.

P. moraviensis showed no significant changes in any growth curve metric (AUC: $p = 0.983$; lag time: $p = 0.476$; max per-capita growth rate: $p = 0.052$; max density: $p = 0.810$). A non-significant trend toward higher maximum per-capita growth rate in polyculture-evolved relative to ancestral lines was observed (Dunn's: $p = 0.052$). *P. moraviensis* did not undergo detectable phenotypic change under the conditions tested here but may have changed along axes not captured by the in vitro growth curve assays.

P. rhodesiae showed significant differences in lag time in both evolved treatments (KW $\chi^2 = 11.47$, $p = 0.003$; Dunn's: monoculture vs. ancestor $p = 0.003$; polyculture vs. ancestor $p = 0.009$), indicating that evolution on tomato seedlings consistently decelerated the onset of growth regardless of community context. In contrast, maximum per-capita growth rate was significantly elevated in monoculture-evolved lines (KW $\chi^2 = 7.06$, $p = 0.029$; Dunn's: monoculture vs. ancestor $p = 0.019$) compared to ancestor.

Species-specific outcomes on bacterial growth on seedlings

In planta bacterial densities did not mirror in vitro performance (**Figure 2E**). *P. syringae* showed a significant overall treatment effect (KW $\chi^2 = 6.27$, $p = 0.044$), driven by monoculture-

evolved lines reaching lower densities than the ancestor (Dunn's $p = 0.020$) despite improved in vitro growth (**Figure 2**). *P. moraviensis* again showed no significant differences (KW $\chi^2 = 1.39$, $p = 0.499$). *P. rhodesiae* polyculture-evolved lines reached higher densities than the ancestor (Dunn's, $p = 0.031$), and this same directional advantage was recovered independently in greenhouse-grown plants, as described below.

Changes in *P. rhodesiae* growth strategy correspond with increased growth on plants

Tomato seedlings were inoculated with ancestral or evolved *P. rhodesiae* and their weights were measured at days 1, 2, 5, and 14 post-inoculations ($n = 168$ total). Seedling weight did not differ at days 1 or 2 (KW $p = 0.57$ and $p = 0.65$, respectively). At day 5, evolution treatment significantly affected seedling weight (KW $\chi^2 = 12.27$, $p = 0.002$): monoculture-evolved lines were associated with significantly heavier seedlings than both the ancestor (~1.6-fold; Dunn's $p = 0.024$) and polyculture-evolved lines (Dunn's $p = 0.011$), while polyculture-evolved lines did not differ from the ancestor (Dunn's $p = 0.81$; **Figure 3A**). By day 14 this difference disappeared ($p = 0.14$), suggesting the growth-promoting effect was transient and specific to early colonization or the loss of potential ancestral bacterial cost to the host (**Figure 3B**). A two-way aligned rank transform ANOVA confirmed that the effect of evolution treatment on seedling weight depended on time since inoculation (treatment × day interaction: $F(6,144) = 3.10$, $p = 0.0069$; treatment main effect $F(2,144) = 0.88$, $p = 0.42$; day $F(3,144) = 9.47$, $p < 0.001$), confirming that the day-5 growth advantage was transient rather than sustained.

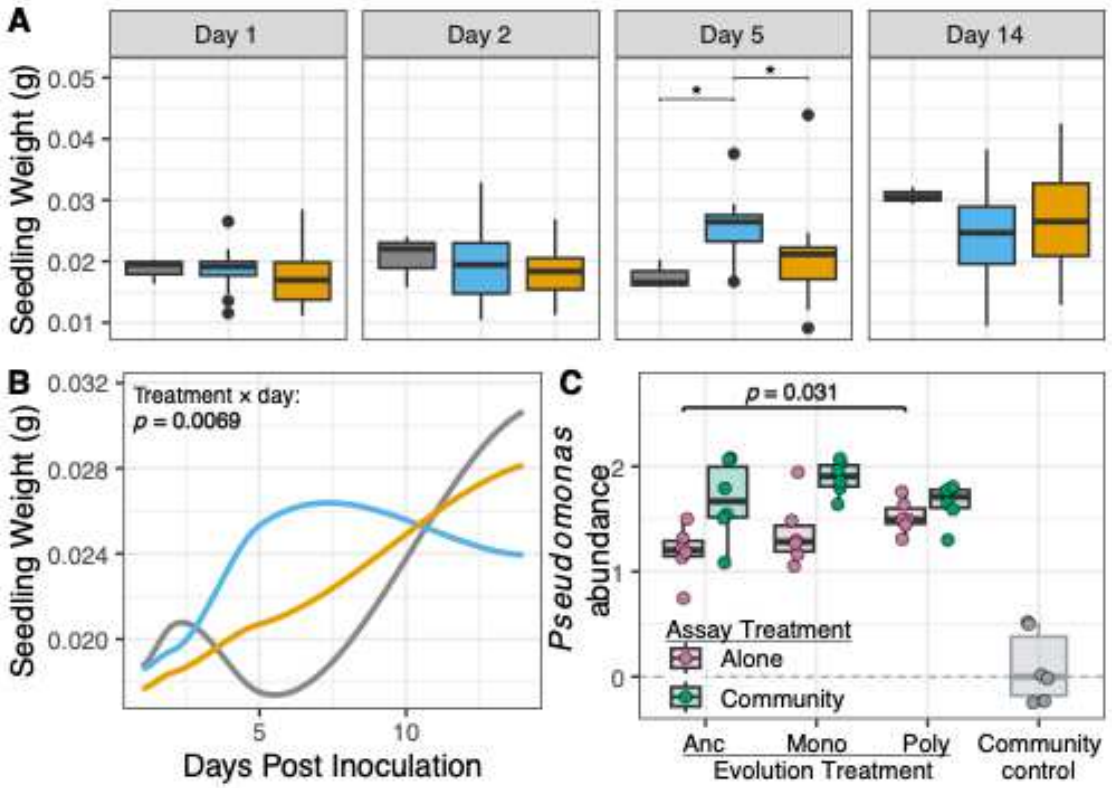


Figure 3. Phenotypic changes in evolved *P. rhodesiae* lines relative to ancestral lines on tomato plants. A) Seedling weight of tomato seedlings inoculated with ancestral (grey), monoculture-evolved (blue), or polyculture-evolved (gold) *P. rhodesiae* SC25. Fresh weight (g) was measured at days 1, 2, 5, and 14 post-inoculation (n = 42 seedlings per timepoint, 168 total). Individual points represent individual seedlings; boxes show median and interquartile range. At day 5, monoculture-evolved lines were associated with significantly heavier seedlings than both the ancestor (Dunn's p = 0.024) and polyculture-evolved lines (Dunn's p = 0.011); no significant differences were detected at days 1, 2, or 14. B) Line plot depicting the changes in seedling weight over time. Line colors denote evolution treatment (grey = ancestor, blue = monoculture, gold = polyculture). **C)** Relative Pseudomonas abundance on greenhouse tomato plants inoculated with ancestral, monoculture-evolved, or polyculture-evolved *P. rhodesiae* SC25. Abundance was quantified by *rpoD* qPCR and expressed as efficiency-corrected fold-difference relative to the community-only control median. Plants were inoculated either alone (red) or alongside a natural phyllosphere community from UC Davis tomato plants (green); grey denotes community-only control plants (n = 6 per group). The dotted line at y = 1 indicates background *Pseudomonas* abundance in community-only controls. All focal treatments established significantly above background (Wilcoxon signed-rank vs. 1.0, all p = 0.016). Among plants inoculated alone, polyculture-evolved lines reached significantly higher *Pseudomonas* abundance than the ancestor (≈1.9-fold; Dunn's p = 0.031).

To discern whether the phenotypic differences among evolved *P. rhodesiae* populations extended beyond the seedling stage, we quantified total *Pseudomonas* abundance on greenhouse-grown tomato plants. Colonization was measured by qPCR for ancestral and evolved *P. rhodesiae* lines inoculated either alone or alongside a natural phyllosphere community isolated from tomato plants grown at the UC Davis Student Farm (**Supplementary Material** and **Figure**

186 **S1**). After correcting for matched community background, all three evolution treatments
187 established significantly above background (Wilcoxon, p = 0.016). Among plants inoculated
188 alone, pairwise comparisons revealed that polyculture-evolved lines reached significantly higher
189 *Pseudomonas* abundance than ancestor inoculated plants (≈1.9-fold; Dunn's p = 0.031), while
190 monoculture-evolved lines did not differ from the ancestor (Dunn's $p = 0.55$; **Figure 3C**).
191 Notably, this is the same directional result obtained independently in the seedling colonization
192 assay (**Figure 2E**). Under co-inoculation with the natural community, all lines maintained
193 comparably high colonization, however, abundance did not differ among evolution treatments
194 (KW p = 0.182; **Figure 3C**). Strain-specific rifampicin-selective CFU plating was directionally
195 concordant but not significant (**Supplementary Figure S2** and **Tables S1-S2**). Altogether,
196 evolution in a community context increased *P. rhodesiae* colonization success.
197
198 Increased in vitro growth in *P. syringae* did not correspond with enhanced virulence in planta
199 To assess changes in pathogenicity of evolved lines, disease severity was scored and
200 summarized as area under the disease progression curve (AUDPC). Disease scores differed
201 significantly across evolutionary backgrounds (**Figure 4A**; KW p = 0.015). When inoculated
202 either alone or with the SynCom, *P. syringae* evolved under monoculture conditions caused
203 significantly less disease than the ancestral genotype (Dunn's: ancestor vs. monoculture p =
204 0.015; **Figure 4B).** Monoculture-evolved populations varied considerably in virulence. Two
205 populations (DC02 and DC04) caused no detectable disease when inoculated alone, and a third
206 (DC03) caused negligible disease scoring a maximum mean of 0.33. DC04, however, was
207 attenuated only in the absence of the community, reaching the highest disease burden of any
208 monoculture-evolved population when co-inoculated with the SynCom (AUDPC = 7.00),
209 whereas DC02 and DC03 remained attenuated in both contexts. This reduction in virulence in

the monoculture treatment, paired with in vitro growth improvements, raises the possibility of a growth-virulence tradeoff, whereby adaptation to rapid proliferation comes at a cost to in planta pathogenicity traits. Alternatively, passaging in the absence of community members may have relaxed selection for virulence factors that are only relevant when competing or establishing infection under realistic ecological conditions.

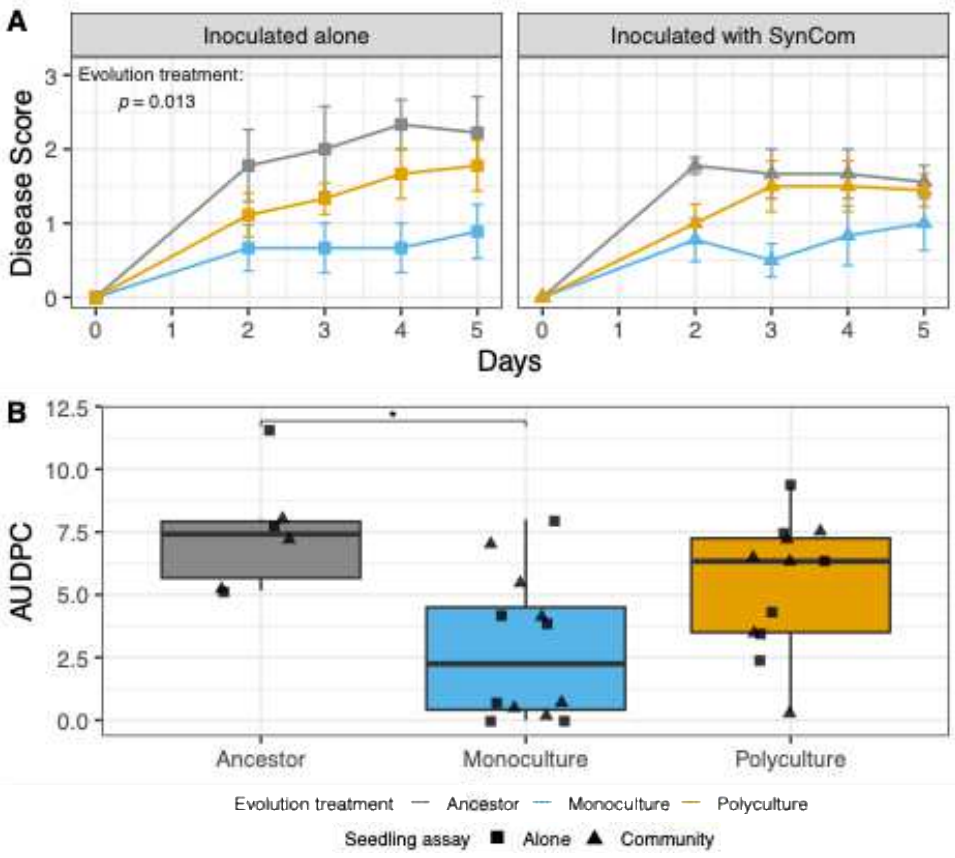


Figure 4. Disease severity of tomato seedlings inoculated with ancestral, monoculture-evolved, or polyculture-evolved *P. syringae* DC3000. **A)** Mean disease score (0–3 scale: 0 = no symptoms, 1 = mild speckling, 2 = extensive speckling/chlorosis, 3 = necrosis/leaf detachment) over five days post-inoculation, shown separately for seedlings inoculated alone (left) or alongside the 14-member SynCom (right). Line color denotes evolution treatment (grey = ancestor, blue = monoculture-evolved, gold = polyculture-evolved); point shape denotes inoculation context (squares = alone, triangles = SynCom). Evolution treatment significantly affected disease burden across both contexts (AUDPC, aligned rank transform ANOVA: $F(2,24) = 5.24$, $p = 0.013$), whereas inoculation context had no detectable effect ($F(1,24) = 0.001$, $p = 0.98$) and did not interact with treatment ($F(2,24) = 0.22$, $p = 0.80$). **B)** Area under the disease progression curve (AUDPC) for each evolution treatment, pooled across inoculation context given the absence of a context effect (6, 12, and 12 populations, respectively). Points represent individual populations, with shape denoting inoculation context; boxes show median and interquartile range.

Genotypic changes were species and treatment specific

Whole-genome sequencing at Passage 6 and Passage 12 identified adaptive mutations underlying the phenotypic changes observed. At Passage 6, mutations were still overwhelmingly segregating (median frequency 13.4%; 8 fixed in total) and fixation did not yet differ between treatments (0.17% vs. 0.30% of mutations ≥85% in monoculture and polyculture; $p = 0.22$), indicating that the divergence in fixation rate reported below emerged during the second half of the experiment. Because target identity was nonetheless largely established by the midpoint, analysis focused on Passage 12 (**Supplementary Material** and **Tables S3–S6**). Mutation analysis of Passage 12 populations first identified 9,879 mutations across all 36 populations at a 5% frequency or higher. After filtering to a 10% frequency threshold with a sliding-window correction, 2,482 mutations remained for downstream analysis (**Extended Data Figure 1** and **Supplementary Table S7**).

Mutations were predominantly located in coding regions (74.4%), consistent with adaptive rather than neutral evolution. The majority of mutations were point mutations (n = 2,376; 95.7%), followed by insertions and deletions (indels; n = 106; 4.3%). *P. syringae* and *P. moraviensis* mutations were mostly nonsynonymous (48.4% and 49.4%, respectively), followed by intergenic changes (26.2% and 26.8%); *P. rhodesiae* instead skewed toward synonymous (24.6%) and frameshift (6.9%) changes (**Figure 5A**). Total mutation counts followed the same gradient in reverse: *P. syringae* carried the fewest (n = 576), while *P. moraviensis* (n = 947) and *P. rhodesiae* (n = 959) accumulated substantially more. Per-isolate mutation counts differed significantly by species (KW $\chi^2 = 9.27$, $p = 0.010$), with *P. syringae* showing the largest treatment disparity (monoculture mean 18.5 vs. polyculture mean 77.5 mutations/isolate; **Figure 5B**; **Extended Data Table 2**).

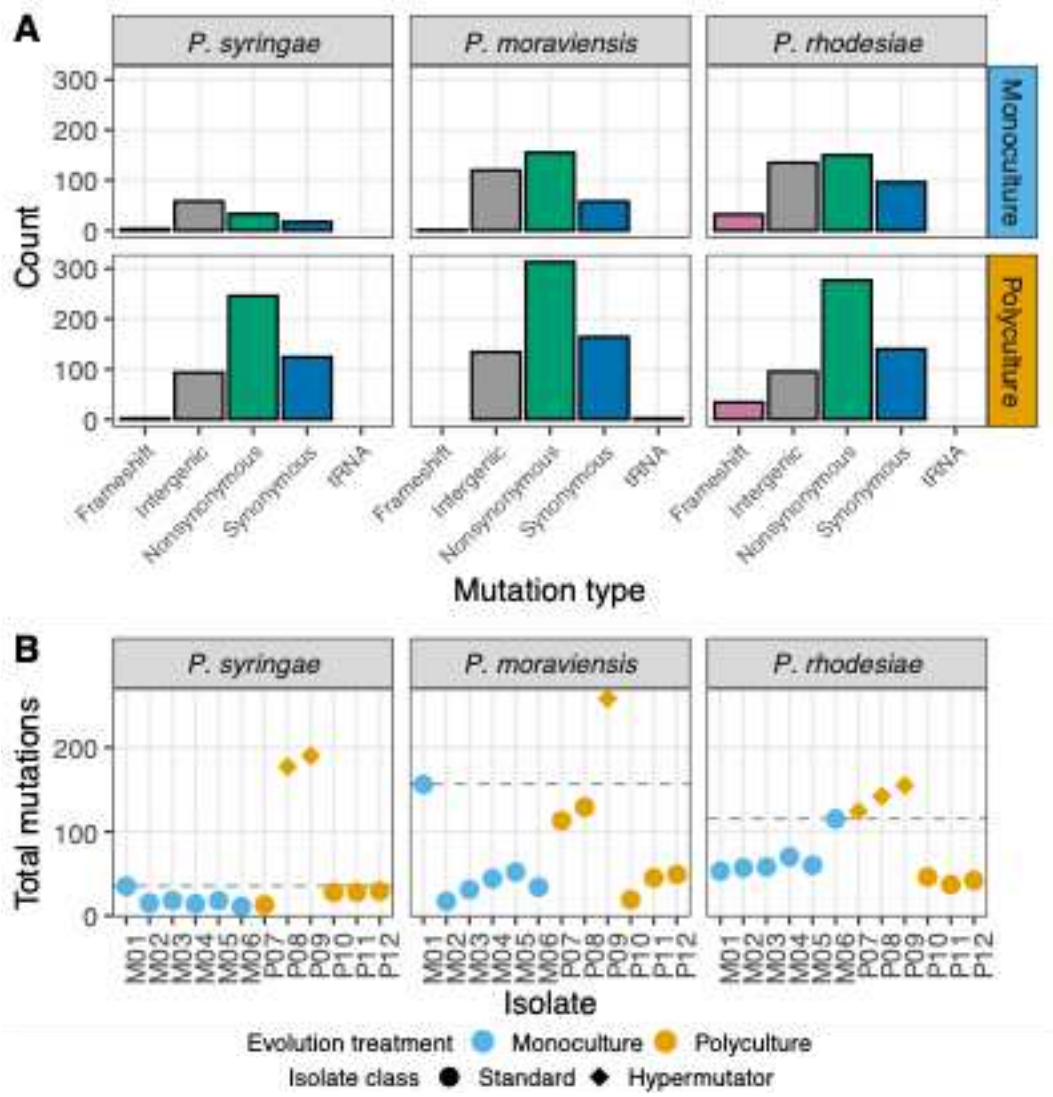


Figure 5. Mutation burden and functional composition across evolved *Pseudomonas* populations at Passage 12. A) Mutation counts by functional class, separated by species (columns) and evolution treatment (rows). Total mutations: *P. rhodesiae* n = 959, *P. moraviensis* n = 947, *P. syringae* n = 576. B) Total mutations (≥10% allele frequency) per isolate, grouped by species, for monoculture-evolved (blue circles) and polyculture-evolved (gold circles) lines. Diamonds mark hypermutator populations, defined as exceeding the monoculture mean + 2 SD threshold within each species (dashed grey line; thresholds: *P. syringae* = 35.5, *P. moraviensis* = 156.8, *P. rhodesiae* = 115.5 mutations). Hypermutator lineages arose exclusively among polyculture-evolved populations (6 of 18 polyculture vs. 0 of 18 monoculture; Fisher's exact test, one-tailed, p = 0.0095). Isolate labels indicate treatment and replicate number (M01–M06 = monoculture, P07–P12 = polyculture).

To investigate the effects of selection history on mutation identity, we compared mutation types across evolution treatments. Mutation type proportions differed significantly between treatments among genic mutations ($\chi^2 = 15.08$, df = 2, $p = 5.3\times10^{-4}$). Expanding to genic

vs. intergenic mutations, polyculture populations showed a higher proportion of genic mutations than monoculture (80.2% vs. 63.5%; $\chi^2 = 81.77$, df = 1, $p < 0.0001$), suggesting community context enhances selection on protein-coding regions. Applying the McDonald-Kreitman (MK) framework (**Extended Data Figure 2**) showed a near-neutral direction of selection (DOS) for *P. syringae* in both conditions (0.007, 0.002), though there were few fixed genic mutations (Dn ≤ 2/group). *P. moraviensis* DOS values were positive in both treatments but significant only in polyculture (monoculture DOS = 0.183, p = 0.108; polyculture DOS = 0.219, p = 0.015), while *P. rhodesiae* showed significant negative DOS in polyculture only (monoculture DOS = -0.115, p = 0.211; polyculture DOS = -0.195, p = 0.033). This same pattern held within MK-eligible mutations at the species level: fixation rate dropped from monoculture to polyculture in all three species (*P. syringae* 6.0% to 0.8%; *P. moraviensis* 8.9% to 6.1%; *P. rhodesiae* 15.9% to 7.9%).

Mutation fixation dynamics and targets of adaptation

Of 2,482 mutations, 221 (8.9%) reached fixation (>85% frequency) and 2,261 (91.1%) remained polymorphic. Monoculture populations fixed mutations at a significantly higher rate than polyculture (12.7% vs. 6.9%; $\chi^2 = 23.34$, $p < 0.0001$), consistent with more complete selective sweeps under the more stable monoculture selective environment, whereas polyculture environments may impose fluctuating or diversifying selection that maintains within-population polymorphism. A total of 101 genes were independently mutated in three or more populations (**Supplementary Table S8** and **Extended Data Figure 3-4**). The most frequently mutated gene was *rpoB* (RNA polymerase β subunit; 37 mutations across 23 independent populations of *P. moraviensis* and *P. rhodesiae* in both treatment conditions), with 36 of 37 mutations reaching fixation (≥85% frequency). Mutations at *rpoB* were predominantly nonsynonymous substitutions

(n = 24) and frameshifts (n = 13). In *P. moraviensis*, *DDIIGDGP_01200* (12 populations, 100% fixed) and *plsB* (phospholipid biosynthesis; 7 populations) were among the most recurrently mutated loci. In *P. rhodesiae*, high-confidence targets included *DDAHOALL_00229* (12 populations, 100% fixed), *rluC/rne* (RNA processing; 12 populations, 100% fixed), and *liuE* (leucine catabolism; 8 populations). In *P. syringae*, parallel evolution was concentrated in intergenic regions, notably *pitA_2/emrA_1* and *OPEHBMIK_04903/OPEHBMIK_04904* (both 11 populations, 100% fixed), consistent with regulatory rather than protein-coding adaptation. The near-exclusive species-specificity of parallel targets, with *rpoB* as the sole high-confidence cross-species exception, suggests strongly divergent adaptive trajectories across the three *Pseudomonas* species.

Comparing fixed mutations across the six monoculture-evolved populations, only DC02 carried unique fixed coding mutations, including a nonsynonymous substitution in *hdfR_2*, a LysR family transcriptional regulator implicated in flagellar and virulence gene regulation in *P. syringae*, representing a strong candidate locus for its avirulent phenotype. The remaining attenuated populations carried no unique fixed coding mutations, suggesting their phenotypes may result from multiple low-frequency polymorphisms or from fixed intergenic mutations.

Putative hypermutator lines were identified as populations exceeding the monoculture mean + 2 standard deviations within each species, providing a baseline mutation rate independent of the treatment being tested. Six of 18 polyculture populations (33.3%) met this criterion versus zero of 18 monoculture populations (Fisher's exact p = 0.0095): two *P. syringae* (P08 and P09; 177-190 mutations), one *P. moraviensis* (P09; 258 mutations), and three *P. rhodesiae* (P07-P09; 124-155 mutations), all exclusively polyculture (**Figure 5B**).

DISCUSSION

Integrating phenotypic and genotypic data across 36 evolved lines, we found that growth improvements were species- and treatment-specific, that in vitro gains did not consistently translate to enhanced in planta outcomes, that polyculture-evolved *Pseudomonas* increased hypermutator lineages, and that parallel evolution at over 100 loci provided genome-wide evidence for positive selection concentrated in largely species-specific targets. Improvements in in vitro growth did not translate into elevated cell densities on seedlings in *P. syringae*, where monoculture-evolved lines showed the greatest laboratory gains yet did not outperform ancestors in planta. Rapid in vitro growth typically demands investment in biosynthetic machinery and ribosome biogenesis, potentially at the expense of host-colonization traits[23]. The genetic basis of virulence attenuation differed between the other attenuated populations: DC02 fixed a candidate regulatory mutation in *hdfR_2*, a LysR-family regulator with known roles in flagellar and virulence control[24], while the other attenuated populations carried no unique fixed coding mutation, pointing to polygenic low-frequency or intergenic mutations contributing to the phenotype that could be explored with gene expression analyses. Adaptation to rapid growth and loss of pathogenicity thus appear to be co-occurring but genetically separable outcomes of monoculture evolution.

Across independent assays, polyculture-evolved *P. rhodesiae* consistently emerged as the strongest colonizer, reaching higher in planta densities than the ancestor on seedlings and higher *Pseudomonas* abundance when inoculated alone in the greenhouse, directionally corroborated by rifampicin-selective CFU plating under an established community. Because a resident community is a competitive barrier to colonization, this pattern is consistent with polyculture passaging selecting for traits that improve establishment under interspecific competition[4]. These

results bear directly on the potential use of *P. rhodesiae* as a microbial amendment. The treatment history that produced the best colonizer (polyculture) was therefore not the one that produced the best host outcome (monoculture), a trade-off between colonization efficacy and host cost that is directly relevant to strain selection, where both establishment and host compatibility determine practical utility.

In contrast, *P. moraviensis* showed no significant phenotypic change across any growth metric or in planta colonization assay, despite a mutation burden statistically indistinguishable from *P. rhodesiae* (947 versus 959 mutations). This genomic-phenotypic discordance may reflect cryptic or neutral variation buffered by genetic redundancy or epistatic compensation, well documented in long-term evolution[25,26]. Still, the species-specific pattern of parallel evolution in *P. moraviensis*, concentrated in transcriptional regulators, phospholipid biosynthesis, and metabolic loci rather than the global regulators dominating the other two species suggest adaptation along a distinct genotypic axis.

The mutation analysis provided strong evidence for positive selection at specific loci: the nonsynonymous-to-synonymous ratio was 2.23 (monoculture) and 1.98 (polyculture), and the 101 genes independently mutated in three or more populations is roughly 30-fold above the neutral-drift expectation. *rpoB* was the single most frequently mutated locus, fixed in 23 of 24 populations across *P. moraviensis* and *P. rhodesiae* but entirely absent in *P. syringae*. We interpret this cautiously. All lines were passaged under continuous rifampicin selection, and *rpoB* is the canonical target of rifampicin resistance[27]. *P. syringae* DC3000 carries innate resistance through a different mechanism, whereas the *P. moraviensis* and *P. rhodesiae* ancestors were themselves made rifampicin-resistant immediately before the experiment, almost certainly via an initial *rpoB* mutation. The recurrent *rpoB* mutations we observe therefore likely reflect, at least

in part, continued optimization or compensation of that induced resistance under sustained antibiotic selection[28], rather than host- or community-driven selection alone. This does not exclude a genuine adaptive role, since RNA polymerase mutations are well-documented general-purpose targets in antibiotic-free evolution experiments [29], but the strength of *rpoB* as evidence for host-associated selection specifically should be weighed against this alternative.

Beyond *rpoB*, parallel evolution converged on *flhA* in *P. rhodesiae* (12 of 12 populations), consistent with the well-documented loss-of-motility trajectory in which non-motile variants outcompete motile ancestors by shedding the energetic cost of flagellar biosynthesis, and possibly reducing chemotaxis-driven competition or phage susceptibility in the community context[30]. BLASTx annotation of hypothetical targets (**Supplementary Table S8**) recovered three further recurring themes: carbon and nutrient acquisition from host-derived substrates; membrane and abiotic-stress adaptation in *P. moraviensis*; and interbacterial competition, with five hypothetical loci across both commensals annotating to Rhs/T6SS toxin components including DddA-family deaminases[31,32]. Notably, one such locus (*DDAHOALL_04353*) appeared exclusively in polyculture-evolved lines, suggesting that community context selected for competitive traits, while the other four appeared in both treatments, suggesting this pressure is not confined to the polyculture environment.

A consistent pattern across axes was that monoculture-evolved lines showed stronger signatures of adaptation, particularly phenotypically: monoculture *P. syringae* and *P. rhodesiae* showed the greatest in vitro gains, monoculture populations had a higher fixation rate (12.7% versus 6.9%), and hypermutator lineages were enriched in polyculture (6 of 18 versus 0 of 18; Fisher's exact $p = 0.0095$). The SynCom likely imposed a more variable, multidimensional selective environment in which no single mutation consistently conferred an advantage, making

383 complete sweeps less likely[33,34]; community members may also have reduced focal effective
384 population size by competing for space and nutrients or increased stress[35]. To distinguish these
385 mechanisms, we suggest direct abundance estimates of microbial members during passaging and
386 manipulation of community diversity.

387 Ecological role along the pathogen-to-PGPB continuum influenced the direction of
388 evolutionary change. *P. syringae* gained in vitro growth while losing virulence through at least
389 two mutational routes; *P. rhodesiae* showed a community-dependent colonization advantage
390 paired with a monoculture-specific reduction in host cost; and *P. moraviensis*, despite a
391 comparable mutation burden, showed no detectable phenotypic change on any axis assayed.
392 Ecological role thus shapes whether and how a species responds to community membership
393 more reliably than it predicts the magnitude of that response. Community context consistently
394 shifted the molecular landscape across all three species by lowering fixation rates, enriching
395 genic mutations, and promoting hypermutators. That the same ancestor, host, and passage regime
396 produced different phenotypic outcomes depending only on whether competitors were present
397 indicates that community context leaves a durable evolutionary legacy, and that adaptation is
398 contingent not just on genetic background[36] but on the ecological history of the lineage.
399 Predicting how plant-associated bacteria evolve under complex agricultural microbiomes will
400 therefore require considering ecological identity, community context, and the selective pressures
401 introduced by the experimental design itself.
402
403 **METHODS**
404 Focal strains and microbial community background

405 The focal bacterial strains whose evolution was directly followed in this study consisted
406 of the plant pathogen *P. syringae* DC3000 and two commensal strains with which to compare
407 and contrast evolutionary outcomes. The commensal strains are *P. moraviensis* SC16 and *P.*
408 *rhodesiae* SC25, both bacterial strains isolated from natural tomato plants. The original wild type
409 ancestral genotypes of all three species have been previously sequenced and described[37]. For
410 community, or polyculture, treatments, we utilized a defined microbial community[38], otherwise
411 known as a synthetic community (SynCom), consisting of 14 bacterial species which were
412 isolated each from tomato plants and the isolation history was previously described in
413 Mehlferber et al. (2023)[11]. Briefly, the SynCom is composed of six Gram-negative and eight
414 Gram-positive bacteria across 10 genera that were selected to reflect a general community of
415 bacteria that exists in the tomato phyllosphere (**Table 1**)[39].
416 We leveraged an antibiotic resistance marker for selection isolation and passaging of the
417 focal strains. *P. syringae* DC3000 is inherently resistant to the antibiotic rifampicin[15] and the
418 community background had no natural resistance to rifampicin. To generate rifampicin resistant
419 ancestors of *P. moraviensis* SC16 and *P. rhodesiae* SC25, we grew the strains in King's B (KB)
420 liquid medium at 28.0°C with 150 RPM for 24 hours. Bacteria from the liquid culture were
421 spread onto KB hard agar plates supplemented with 100 µg/ml of rifampicin. The plates were
422 incubated at 28.0°C for up to 48 hours for colony development. A putative resistant colony was
423 purified on a new KB hard agar plate supplemented with 100 µg/ml of rifampicin and incubated
424 at 28.0°C for 24 hours. To validate culture purity, we sequenced and amplified the 16S rRNA
425 gene with colony PCR using the forward 27F 5'-AGAGTTTGATCCTGGCTCAG-3' and
426 reverse 1492R 5'-GTTACCTTGTTACGACTT-3' primers. We performed 20 µl reactions using
427 Platinum HotStart Master Mix (Invitrogen) with the following cycle conditions: initial

denaturation at 94.0°C for 3 min followed by 30 cycles of denaturation at 94.0°C for 30 sec, annealing at 48.4°C for 30 sec, and extension at 72.0°C for 1 min 30 sec with a final extension at 72.0°C for 10 sec. The UC Berkeley DNA Sequencing Facility performed PCR clean up and Sanger sequencing on the PCR products (https://ucberkeleydnasequencing.com/home). The chromatograms were visualized and sequences extracted using 4peaks (https://nucleobytes.com/4peaks/) and species were verified through BLAST analysis against the 16S rRNA ribosomal sequences database [40]. Frozen glycerol stocks of the verified and purified ancestral bacteria were prepared and stored at -70.0°C.

Synthetic community inoculum preparation

To prepare SynCom inoculum, all 14 SynCom members were grown from frozen in 45 ml of KB liquid medium and incubated at 28.0°C for 48 hours. The bacterial cultures were pelleted by centrifugation for 10 minutes at 2500 rcf and the supernatant was poured off. Each pellet was resuspended and the optical density at 600nm (OD_{600}) of each culture was measured using a Tecan spectrophotometer (Infinite F50) and was normalized using sterile KB media. Using the normalized OD_{600} of each sample, the volume necessary of each sample to yield an equal ratio of each species was calculated. The SynCom suspension was vortexed well and stored in glycerol at -70.0°C.

Seed sterilization and germination

Tomato seeds (*S. lycopersicum* cv. 'Moneymaker') were rinsed with 70% ethanol for one minute, surface sterilized in 2.7% bleach (sodium hypochlorite) and 0.00027% Tween-20 solution for 20 minutes, then washed three times with sterile MilliQ water to remove residual

bleach. Each seed was placed in a sterile 15 ml tube with 7 ml of 1% water agar sealed with AeraSeal film to facilitate gas exchange. The tubes were maintained in a 21.0°C chamber in the dark until shoot emergence, then moved to a 24.0°C growth chamber with a 15-hour day:9-hour night cycle until inoculation twelve days post-sterilization.

Experimental evolution *in planta*

The evolution experiment consisted of two treatments: a focal bacterium passaged alone or passaged with a SynCom biotic background on tomato seedlings (**Figure 1**). There were six replicates per treatment, and each treatment was conducted for all three *Pseudomonas* species (*P. syringae*, *P. moraviensis*, and *P. rhodesiae*) for a total of 36 evolving lines. To begin the evolution experiment, all three ancestral *Pseudomonas* species were grown on KB hard agar plates supplemented with rifampicin and a single colony was selected to begin each line. The colonies were suspended in KB liquid medium supplemented with rifampicin and incubated for 24 hours at 28.0°C. On inoculation day, the frozen SynCom stock was quickly thawed, and the entire volume was aliquoted into a microcentrifuge tube. The SynCom stock and focal bacteria cultures were pelleted at 3,500g and washed with 10 mM $MgCl_2$ to remove residual media or glycerol. Inocula were prepared by resuspending pellets in 10 mM $MgCl_2$ to a bacterial OD_{600} of 0.002 and adding 0.015% of the surfactant Silwet L-77 to facilitate leaf colonization. For treatment 1 (monoculture), 12-day old seedlings were inoculated with a single species of bacteria. For treatment 2 (polyculture), the normalized focal bacteria were first mixed with the SynCom to generate a 1:1 mixture before inoculation onto the 12-day old seedlings. At each passage, three seedlings were inoculated with sterile 10 mM $MgCl_2$ buffer to serve as

contamination controls. The inoculated seedlings were resealed with breathable film and kept in the 24.0°C growth chamber for 5 days.

Following incubation in the growth chamber, the seedlings were removed from the agar using sterile forceps and the roots were removed using sterilized scissors. The seedlings were placed into sterile 2 ml FastPrep tubes (MP Biomedicals) with a sterile ceramic bead and 10 mM $MgCl_2$. The plant material was homogenized in a FastPrep-24 5 G system (MP Biomedicals catalogue no. 116005500) at 4 m/s for 60 s to homogenize plant tissue. Leaf homogenate was diluted and plated on rifampicin-supplemented KB hard agar plates. For each experimental evolution line (36 lines), 100 colonies were individually picked from plates, mixed and grown overnight to generate inocula for the following generation of seedlings and for long term storage at -70.0°C in glycerol. This was repeated for 12 passages for all three species, and the evolved bacteria were saved at each passage resulting in n = 432 evolved populations. For all of the following assays, Passage 12 populations (referred to as P12, n = 36) were investigated.

Bacterial phenotypic assays *in vitro* and *in planta*

To assess phenotypic change after the evolution experiment, growth curve assays were performed for all 36 evolved lines after 12 passages. We measured the *in vitro* growth rates of the evolved and ancestral lines at 28.0°C in KB liquid media for 72 hours. Evolved and ancestral lines were randomly distributed across the 96-well plate in duplicate for all evolved lines within a single plate and in triplicate for ancestral genotypes. To track the growth, we took OD_{600} measurements every 15 minutes with a 10 sec orbital shaking step prior to each measurement using a Tecan spectrophotometer. The bacterial growth curves were analyzed using the R

495 package gcplyr in Rstudio [41,42]. The area under the curve (AUC), lag time, doubling time, and
496 maximum density were all calculated from the growth curve data.
497 To assess phenotypic changes in planta, we measured the final bacterial cell densities on
498 the seedlings for all ancestral and evolved lines and disease progression specifically for all *P.*
499 *syringae* DC3000 ancestral and evolved lines. We inoculated 12-day old seedlings with the
500 evolved or ancestral lines alone following previously described methods. A set of seedlings
501 (n=3) were inoculated with sterile $MgCl_2$ buffer alone and handled identically alongside
502 ancestral and evolved lines at each timepoint to provide an uninoculated growth baseline and
503 contamination controls. The seedlings with bacteria were kept in the growth chambers for 5 days
504 and homogenized as described above. We performed serial dilutions with the homogenate, plated
505 all dilutions, and counted the resulting colonies. Symptom development was tracked in the
506 growth chambers and disease progression was scored as follows: no symptoms (level 0), mild
507 speckling (level 1), extensive speckling and/or chlorosis (level 2) and leaf necrosis and/or
508 detachment (level 3) [10].
509
510 Genome sequencing of evolved populations
511 After the evolution experiment, the rifampicin resistant ancestors as well as the halfway
512 point (Passage 6 or P06) and final end-point populations (Passage 12 or P12) were sequenced to
513 identify variants arising from the evolution regimes. We revived populations from 100 µl of
514 frozen glycerol stock in 5 ml of KB liquid media. The cultures were incubated at 28.0°C with
515 150 RPM for 8-12 hours to capture the populations prior to the cultures reaching stationary phase
516 and for any selective processes to proceed. We extracted the DNA from 36 evolved populations
517 using the Qiagen Blood and Tissue Kit for DNA Extraction. The genomic DNA concentration

518 was quantified using Qubit dsDNA HS assay kits. The DNA was prepared for short read
519 sequencing using the Illumina DNA Prep kit. The Illumina libraries were each uniquely
520 barcoded, multiplexed, and sequenced using the Illumina NextSeq 2000 P2 at the Chan-
521 Zuckerberg Biohub in San Francisco. The ancestral genomes of *P. moraviensis, P. rhodesiae*,
522 and *P. syringae* were previously sequenced, assembled, and described[37]. The short read sequence
523 quality was assessed with FastQC and MultiQC [43,44]. The reads were trimmed using fastp to
524 remove low quality reads and bases [45]. Passage 6 and Passage 12 were sequenced at two
525 independent timepoints. Each population had an average sequencing depth of approximately
526 290× and 400× coverage (**Supplementary Table S9**) across the chromosome for passage 6 and
527 passage 12, respectively, which was quantified using BBmap [46].
528
529 Variant Detection and Analysis
530 We detected mutations and their respective frequencies in each evolved population using
531 breseq v. 0.35.5 [47] to identify high quality variants in the populations. We performed the breseq
532 analysis in polymorphism mode using the appropriate ancestral genome. Following similar
533 methods, mutations were filtered to exclude highly polymorphic regions, defined as ≥5 mutations
534 within a 200 bp sliding window within a population [10]. Additionally, genes harboring ≥5
535 mutations within a single isolate were excluded to remove putative repetitive or hypervariable
536 loci. Mutations were classified as genic or intergenic, and genic mutations were further assigned
537 as nonsynonymous, synonymous, or frameshift. Comparisons of genic mutation class
538 composition between evolution treatments used a Pearson χ^2 test. tRNA mutations (n = 2, both in
539 polyculture) were excluded from this comparison because their expected cell counts fell below
540 five, violating the χ^2 approximation.

To investigate the putative function of hypothetical proteins among the most frequently mutated genes, we performed BLASTx searches against the Swiss-Prot/UniProtKB database and the NCBI non-redundant (nr) protein database using BLAST+ v2.14.1[40]. Nucleotide sequences of hypothetical protein-coding genes were translated in all six reading frames and queried with an E-value threshold of 1×10^{-5}, a word size of 3, and low-complexity filtering enabled. Up to 10 target sequences per query were retained. Functional annotations were assigned based on consistency of hits across the top results.

To characterize the nature of selection acting on evolved populations, we applied a McDonald-Kreitman (MK) framework[48] restricted to nonsynonymous and synonymous point mutations in coding regions. Mutations were classified as fixed (≥85% allele frequency) or polymorphic (<85%) consistent with our fixation threshold. The Direction of Selection (DOS = Dn/(Dn+Ds) − Pn/(Pn+Ps)) and Neutrality Index (NI = (Pn/Ps)/(Dn/Ds)) were calculated for each species-treatment combination, where positive DOS and NI < 1 indicate positive selection[49]. Statistical significance was assessed by Fisher's exact test and 95% bootstrap confidence intervals were generated from 1,000 resampling iterations per group.

Greenhouse experimentation and qPCR to assess *P. rhodesiae* colonization

To investigate the context dependence in the phenotypic changes identified in *P. rhodesiae*, we conducted an experiment in the greenhouse with juvenile tomato plants. We grew tomato plants from sterilized seeds, as previously described, in water agar until the cotyledon emerged. Following germination, we transplanted the seedlings to seedling trays filled with sterilized calcined clay, maintained in the growth chambers, and watered with sterile water supplemented with Hoagland's solution (1.6 g/L). Once the seedlings were about 10-12 cm tall

564 and true leaves developed, we transplanted the seedlings to individual pots with soil and
565 maintained in a greenhouse at the Oxford Tract research growing facilities at UC Berkeley
566 (**Supplementary Figure S1**). In the greenhouse, we inoculated the plants with either a natural
567 phyllosphere microbiome collected from sonicated tomato leaf material collected from the
568 Student Farm at UC Davis or sterile $MgCl_2$ buffer solution. The plants were sprayed weekly for
569 three weeks, and a single leaflet was taken from each plant, homogenized, and plated each week
570 for CFU counting to assess colonization progress.

571 We compared the colonization ability of evolved and ancestral *P. rhodesiae* on the
572 tomato plants in the greenhouse. We prepared *P. rhodesiae* inoculum to an OD_{600} of 0.02. Each
573 evolved and ancestral *P. rhodesiae* line was sprayed onto a plant that was previously inoculated
574 with the community and a plant that was sprayed with sterile buffer. In total, we maintained 42
575 plants, including control plants inoculated with just the natural communities and sprayed with
576 sterile buffer instead of *P. rhodesiae*. Strain-specific colonization was assessed by rifampicin-
577 selective CFU plating (see **Supplementary Material**).

578 We further investigated the colonization ability quantitative PCR (qPCR) on DNA
579 extracts from the harvested plants. We harvested the entire above-ground parts of the tomato
580 plants by excising them from their base using ethanol-sterilized scissors, transferred to 1-gallon
581 plastic bags, and transported on ice to the laboratory. Plant weight was recorded and foliar
582 bacteria were collected from the plant material by adding 250 ml of sterile $MgCl_2$ to the sample
583 bags and sonicating for 20 min in a water bath (Branson model 5800). The sonicate was filtered
584 through autoclaved coffee filters, collected into 50 ml conical tubes, and centrifuged at 4200 rcf
585 for 10 min to pellet microbial cells. The supernatants were decanted from each tube, and the

pellets were frozen at −80.0°C for subsequent DNA extractions. DNA extractions on community pellets were performed with the Qiagen DNeasy Powersoil Pro kit.

To quantify *P. rhodesiae* colonization, we used qPCR with primers designed for the *rpoD* gene which amplifies *Pseudomonas* specifically [50]. We used the primers *rpoD*-F 5'-AAGCCAGCAGCGACGATGAAGAAG-3' and *rpoD*-R 5'-GGCCTTGCGGGTGATTTCCATTTG-3'. We performed reactions using PowerTrack SYBRgreen (Applied Biosystems) with the cycle conditions: initial denaturation at 95.0°C for 2 min followed by 40 cycles of denaturation at 95.0°C for 30 sec, annealing and extension at 60.0°C for 30 sec.

Pseudomonas colonization qPCR analysis

Cycle threshold values were determined in StepOne software v2.3, with each sample assayed in technical triplicate and outlier replicates removed prior to averaging; all DNA templates were normalized to 1.5 ng/µL input, and samples distributed across two plates with a shared inter-plate calibrator. Amplification efficiency was estimated from a standard curve of serially diluted *P. rhodesiae* genomic DNA (efficiency = 93.5%, slope = −3.49, $R^2 > 0.99$), and relative *Pseudomona*s abundance per sample was expressed as the efficiency-corrected fold-difference from the community-only control. For community-inoculated plants, abundance was normalized by dividing each focal sample by the relative abundance of its paired community-only control, yielding fold-abundance above the community *Pseudomonas* background.

Statistical Analyses and Visualization

All statistical analyses were performed in R v 4.0.2 [41]. We utilized rstatix and tidyverse for summarizing statistical analyses [51,52]. Two-way ANOVAs were used to test interaction terms, and for the seedling weight and AUDPC analysis, the ARTool was used[53]. For statistical analysis where normality was not met, we utilized the Kruskal-Wallis tests with the dunn.test package in R for non-parametric analysis. Figure preparation was performed with ggplot2, cowplot, and ggpubr [54] in Rstudio, edits performed with Adobe Illustrator, and BioRender.com was used for the experimental design schematic.

DATA AVAILABILITY STATEMENT

Raw sequencing data of the ancestral and evolved lines are available at the NCBI SRA at PRJNA1496971.

ACKNOWLEDGEMENTS

T.N.B was supported by the National Science Foundation (NSF) Postdoctoral Research Fellowship in Biology (#2209111), the San Francisco Chan-Zuckerberg Biohub, and the Gordon and Betty Moore Foundation. J.O.C. was supported by the NSF Bay Area RaMP Program (#2216550). This research used the Savio computational cluster resource provided by the Berkeley Research Computing program at the University of California, Berkeley supported by the UC Berkeley Chancellor, Vice Chancellor for Research, and Chief Information Officer.

REFERENCES

1. Parker, I. M. & Gilbert, G. S. The Evolutionary Ecology of Novel Plant-Pathogen Interactions. *Annual Review of Ecology, Evolution, and Systematics* **35**, 675–700 (2004).

2. Batarseh, T. N. & Koskella, B. Distinguishing among evolutionary and ecological processes shaping microbiome dynamics. *The ISME Journal* wraf107 (2025) doi:10.1093/ismejo/wraf107.
3. Kivikoski, M. *et al.* Evolution induced state shifts in a long-term microbial community experiment. *Proceedings of the National Academy of Sciences* **123**, e2533269123 (2026).
4. Montbel, V. & Hrcek, J. Experimental evolution in communities: beyond pairwise interactions. *Evol* **80**, 889–901 (2026).
5. Kawecki, T. J. *et al.* Experimental evolution. *Trends in Ecology & Evolution* **27**, 547–560 (2012).
6. Metcalf, C. J. E. & Koskella, B. Protective microbiomes can limit the evolution of host pathogen defense. *Evol Lett* **3**, 534–543 (2019).
7. Baumgartner, M., Bayer, F., Pfrunder-Cardozo, K. R., Buckling, A. & Hall, A. R. Resident microbial communities inhibit growth and antibiotic-resistance evolution of *Escherichia coli* in human gut microbiome samples. *PLoS Biol* **18**, e3000465 (2020).
8. Barroso-Batista, J. *et al.* Specific Eco-evolutionary Contexts in the Mouse Gut Reveal *Escherichia coli* Metabolic Versatility. *Current Biology* **30**, 1049-1062.e7 (2020).
9. Stevens, E. J. *et al.* Within-host competition causes pathogen molecular evolution and perpetual microbiota dysbiosis. *ISME J* **19**, wraf071 (2025).
10. Debray, R., Conover, A., Zhang, X., Dewald-Wang, E. A. & Koskella, B. Within-host adaptation alters priority effects within the tomato phyllosphere microbiome. *Nat Ecol Evol* 1–7 (2023) doi:10.1038/s41559-023-02040-w.
11. Mehlferber, E. C. *et al.* Phyllosphere microbial associations improve plant reproductive success. *Frontiers in Plant Science* **14**, (2023).

12. Mehlferber, E. C. *et al.* Polyploidy and microbiome associations mediate similar responses to pathogens in Arabidopsis. *Current Biology* **32**, 2719-2729.e5 (2022).
13. Sarver, E., González-Morelo, K. J., Christensen, K. G., Lefevers, H. M. & Corbin, K. R. Phyllosphere synthetic microbial communities: a new frontier in plant protection. *BMC Plant Biol* **25**, 949 (2025).
14. Silby, M. W., Winstanley, C., Godfrey, S. A. C., Levy, S. B. & Jackson, R. W. *Pseudomonas* genomes: diverse and adaptable. *FEMS Microbiol Rev* **35**, 652–680 (2011).
15. Cuppels, D. A. Generation and Characterization of Tn5 Insertion Mutations in *Pseudomonas syringae* pv. tomato. https://journals.asm.org/doi/epdf/10.1128/aem.51.2.323-327.1986 (1985) doi:10.1128/aem.51.2.323-327.1986.
16. Buell, C. R. *et al.* The complete genome sequence of the *Arabidopsis* and tomato pathogen *Pseudomonas syringae* pv. tomato DC3000. *Proc Natl Acad Sci U S A* **100**, 10181–10186 (2003).
17. Ye, S. *et al.* Biocontrol potential of *Pseudomonas rhodesiae* GC-7 against the root-knot nematode *Meloidogyne graminicola* through both antagonistic effects and induced plant resistance. *Front Microbiol* **13**, 1025727 (2022).
18. Rolón-Cárdenas, G. A., Arvizu-Gómez, J. L., Pacheco-Aguilar, J. R., Vázquez-Martínez, J. & Hernández-Morales, A. Cadmium-tolerant endophytic *Pseudomonas rhodesiae* strains isolated from *Typha latifolia* modify the root architecture of *Arabidopsis thaliana* Col-0 in presence and absence of Cd. *Braz J Microbiol* **52**, 349–361 (2021).
19. Miller, N. T. *et al.* Draft genome sequence of *Pseudomonas moraviensis* strain Devor implicates metabolic versatility and bioremediation potential. *Genomics Data* **9**, 154–159 (2016).

20. Hassan, T. U., Bano, A. & Naz, I. Alleviation of heavy metals toxicity by the application of plant growth promoting rhizobacteria and effects on wheat grown in saline sodic field. *International Journal of Phytoremediation* **19**, 522–529 (2017).
21. Beiki, F. *et al.* New *Pseudomonas* spp. Are Pathogenic to Citrus. *PLOS ONE* **11**, e0148796 (2016).
22. Oueslati, M. *et al.* Diversity of pathogenic *Pseudomonas* isolated from citrus in Tunisia. *AMB Expr* **10**, 198 (2020).
23. Scott, M. & Hwa, T. Shaping bacterial gene expression by physiological and proteome allocation constraints. *Nat Rev Microbiol* **21**, 327–342 (2023).
24. Yamamoto, K. *et al.* LysR-Type Transcriptional Regulator Contributes to *Pseudomonas cannabina* pv. alisalensis Virulence by Regulating Type Three Secretion System. *Bacteria* **3**, 499–512 (2024).
25. Tenaillon, O. *et al.* Tempo and mode of genome evolution in a 50,000-generation experiment. *Nature* **536**, 165–170 (2016).
26. Wiser, M. J., Ribeck, N. & Lenski, R. E. Long-Term Dynamics of Adaptation in Asexual Populations. *Science* **342**, 1364–1367 (2013).
27. Alifano, P., Palumbo, C., Pasanisi, D. & Talà, A. Rifampicin-resistance, *rpoB* polymorphism and RNA polymerase genetic engineering. *J Biotechnol* **202**, 60–77 (2015).
28. Brandis, G. & Hughes, D. Mechanisms of fitness cost reduction for rifampicin-resistant strains with deletion or duplication mutations in rpoB. *Sci Rep* **8**, 17488 (2018).
29. Tenaillon, O. *et al.* The Molecular Diversity of Adaptive Convergence. *Science* **335**, 457–461 (2012).

30. Wang, J. *et al.* Adapted evolution towards flagellar loss in *Pseudomonas syringae*. *Microbiological Research* **290**, 127969 (2025).
31. Alcoforado Diniz, J. & Coulthurst, S. J. Intraspecies Competition in *Serratia marcescens* Is Mediated by Type VI-Secreted Rhs Effectors and a Conserved Effector-Associated Accessory Protein. *Journal of Bacteriology* **197**, 2350–2360 (2015).
32. Wohlfarth, J. C., Ward, D., Pereira, J. & Basler, M. The type VI secretion system and associated effector proteins. *Nat Rev Microbiol* **24**, 288–303 (2026).
33. Hall, J. P. J., Harrison, E. & Brockhurst, M. A. Competitive species interactions constrain abiotic adaptation in a bacterial soil community. *Evol Lett* **2**, 580–589 (2018).
34. Scheuerl, T. *et al.* Bacterial adaptation is constrained in complex communities. *Nat Commun* **11**, 754 (2020).
35. Foster, P. L. Stress-induced mutagenesis in bacteria. *Crit Rev Biochem Mol Biol* **42**, 373–397 (2007).
36. Batarseh, T. N., Batarseh, S. N., Rodríguez-Verdugo, A. & Gaut, B. S. Phenotypic and Genotypic Adaptation of *Escherichia coli* to Thermal Stress is Contingent on Genetic Background. *Molecular Biology and Evolution* **40**, msad108 (2023).
37. Batarseh, T. N. *et al.* Linking genomic and phenotypic traits to interaction outcomes in a synthetic phyllosphere community. 2026.01.16.699983 Preprint at https://doi.org/10.64898/2026.01.16.699983 (2026).
38. Koch, H. *et al.* From “synthetic” to defined microbial communities for clearer terminology. *Nat Commun* **17**, 5283 (2026).
39. Runge, P., Ventura, F., Kemen, E. & Stam, R. Distinct Phyllosphere Microbiome of Wild Tomato Species in Central Peru upon Dysbiosis. *Microb Ecol* **85**, 168–183 (2023).

40. Camacho, C. *et al.* BLAST+: architecture and applications. *BMC Bioinformatics* **10**, 421 (2009).
41. R Core Team. R: A language and environment for statistical computing. (2019).
42. Blazanin, M. gcplyr: an R package for microbial growth curve data analysis. *BMC Bioinformatics* **25**, 232 (2024).
43. Andrews, S. FastQC: A Quality Control Tool for High Throughput Sequence Data. (2010).
44. Ewels, P., Magnusson, M., Lundin, S. & Käller, M. MultiQC: summarize analysis results for multiple tools and samples in a single report. *Bioinformatics* **32**, 3047–3048 (2016).
45. Chen, S., Zhou, Y., Chen, Y. & Gu, J. fastp: an ultra-fast all-in-one FASTQ preprocessor. *Bioinformatics* **34**, i884–i890 (2018).
46. Bushnell, B. BBMap: A Fast, Accurate, Splice-Aware Aligner. https://escholarship.org/uc/item/1h3515gn (2014).
47. Barrick, J. E. *et al.* Identifying structural variation in haploid microbial genomes from short-read resequencing data using breseq. *BMC Genomics* **15**, 1039 (2014).
48. McDonald, J. H. & Kreitman, M. Adaptive protein evolution at the Adh locus in *Drosophila*. *Nature* **351**, 652–654 (1991).
49. Stoletzki, N. & Eyre-Walker, A. Estimation of the Neutrality Index. *Mol Biol Evol* **28**, 63–70 (2011).
50. Lauritsen, J. G. *et al.* Identification and Differentiation of Pseudomonas Species in Field Samples Using an *rpoD* Amplicon Sequencing Methodology. *mSystems* **6**, 10.1128/msystems.00704-21 (2021).
51. Wickham, H. *et al.* Welcome to the Tidyverse. *Journal of Open Source Software* **4**, 1686 (2019).

52. Kassambara, A. rstatix: Pipe-Friendly Framework for Basic Statistical Tests. (2023).
53. Wobbrock, J. O., Findlater, L., Gergle, D. & Higgins, J. J. The aligned rank transform for nonparametric factorial analyses using only anova procedures. in *Proceedings of the SIGCHI Conference on Human Factors in Computing Systems* 143–146 (Association for Computing Machinery, New York, NY, USA, 2011). doi:10.1145/1978942.1978963.
54. Wickham, H. *Ggplot2*. (Springer International Publishing, Cham, 2016). doi:10.1007/978-3-319-24277-4.

Supplementary Files

This is a list of supplementary files associated with this preprint. Click to download.

- 20260812EvoExp1SupplementaryTables.xlsx
- 20260812SupplementaryMaterialMethodsResults.docx